N94- 35622

Tracking System Options for Future Altimeter Satellite Missions

G. W. Davis, H. J. Rim , J. C. Ries, and B. D. Tapley
The University of Texas at Austin/Center for Space Research
2901 North I.H. 35, Suite 300
Austin, TX 78722

Abstract

Follow-on missions to provide continuity in the observation of the sea surface topography once the successful TOPEX/POSEIDON (T/P) oceanographic satellite mission has ended are discussed. Candidates include orbits which follow the ground tracks of T/P, GEOSAT or ERS-1. The T/P precision ephemerides, estimated to be near 3 cm root-mean-square, demonstrate the radial orbit accuracy that can be achieved at 1300 km altitude. However, the radial orbit accuracy which can be achieved for a mission at the 800 km altitudes of GEOSAT and ERS-1 has not been established, and achieving an accuracy commensurate with T/P will pose a great challenge. This investigation focuses on the radial orbit accuracy that can be achieved for a mission in the GEOSAT orbit. Emphasis is given to characterizing the effects of force model errors on the estimated radial orbit accuracy, particularly those due to gravity and drag. The importance of global, continuous tracking of the satellite for reduction in these sources of orbit error is demonstrated with simulated GPS tracking data. A gravity tuning experiment is carried out to show how the effects of gravity error may be reduced. Assuming a GPS flight receiver with a full-sky tracking capability, the simulation results indicate that a 5 cm radial orbit accuracy for an altimeter satellite in GEOSAT orbit should be achievable during low-drag atmospheric conditions and after an acceptable tuning of the gravity model.

Introduction

The very successful TOPEX/POSEIDON (T/P) oceanographic satellite mission has demonstrated the ability to monitor the Earth's sea surface topography from space with very high accuracy (Fu et al., 1994). The radial orbit accuracy of the T/P precise orbit ephemeris is estimated to be 3-4 cm root-mean-square (rms), which is more than a factor of three better than the mission objective (Tapley et al., 1994, Nerem et al., 1994). With the end of the T/P mission in 1997, continuous, high precision observations of the sea surface will be interrupted. Studies of long term variations in the sea surface topography, particularly those related to global change, will thus be negatively impacted. As a result, the oceanographic community has recommended a follow-on mission to provide continuity in the observation of the sea surface topography.

To link new altimeter observations to existing data sets, it is useful to select an orbit which follows the ground track of a previous altimeter mission, such as GEOSAT, ERS-1 or T/P. If continuous, high accuracy monitoring of the sea surface is desired, then a logical choice would be the T/P orbit. The unprecedented accuracy of the T/P orbit ephemeris is due to the extensive force model development efforts, the robust and precise tracking provided by satellite laser ranging (SLR) and the French doppler tracking system DORIS (Nouel et al., 1988), and the low atmospheric drag associated with the 1300 km altitude. Combined with the 2 cm precision of the TOPEX altimeter, it is an ideal platform from which to study the temporal evolution of the ocean circulation. A follow-on mission in the T/P orbit would provide the long term, contiguous observations needed to study such phenomena as the secular increase in mean sea level. To date, over fifty ten-day repeat cycles of TOPEX altimeter data have been collected, and by the projected mission end the data set will span five years. A follow-on mission in the T/P orbit would expand this time frame, making it the preeminent altimeter data set for oceanographic studies.

Another mission option under consideration is the GEOSAT orbit. With a 108° orbit inclination, a greater altimeter coverage of the polar regions is provided. This would allow more complete study of the circumpolar currents and the ice fields. Although the GEOSAT altimeter data set is of lower quality than the T/P data set, it has been studied extensively and can still provide many opportunities for long term studies. The 800 km altitude of the GEOSAT orbit, however, results in increased drag and geopotential perturbations on the satellite, making it

difficult to obtain an orbit with the T/P precision. The orbit errors associated with the geopotential can be reduced to some extent by tuning the gravity field with tracking data from the first few months of the mission, but the orbit errors due to atmospheric drag will be more difficult to overcome. Such effects will be exacerbated by the expected increase in solar activity in the late 1990's. The ERS-1 orbit would have similar modeling problems, with possible additional difficulties due to the sun synchronous orbit.

To illustrate some of the problems already encountered with these altimeter missions, the current estimate of the GEOSAT radial orbit accuracy is 14 cm rms (Chambers et al., 1994). The low accuracy of this orbit relative to the T/P orbit results primarily from the mismodeling of the accelerations due to gravity and drag at low altitudes, but it also results from the noise level of the doppler tracking systems supporting the satellite (primarily U.S. Navy OPNET tracking plus some French, Canadian and Belgian TRANET tracking). These systems have instrument noise levels that are an order of magnitude larger than that of DORIS, the doppler tracking system on T/P, and their measurement noise contributes to the uncertainty in the GEOSAT orbit. Similarly, the estimated radial orbit accuracy of the ERS-1 orbit is on the order of 10 cm rms (Kozel et al., 1994). Due to the failure of PRARE on ERS-1, only a limited amount of SLR tracking data is available for the ERS-1 orbit computation and efforts are being made to supplement the SLR tracking with dual satellite cross-over measurements that take advantage of the precise T/P orbit. The use of altimeter information for orbit improvement, however, can lead to aliasing of oceanographic signal into the orbit. It is thus important that a tracking system that consistently produces well distributed, high precision observations of the satellite motion be available to support future missions with low altitude orbits such as GEOSAT and ERS-1.

The T/P experience has shown that tracking data from a combination of SLR and DORIS or from the Global Positioning System (GPS) can be used to obtain independent orbits that agree with each other at the 2-3 cm level. To illustrate the success of the T/P orbit determination effort, a revised orbit error budget is provided in Table 1. It is observed that the pre-launch sources of orbit error have been substantially reduced, resulting in an overall radial orbit accuracy that is more than three times lower than that of GEOSAT or ERS-1. If a follow-on mission occupies the T/P orbit, it is very likely that this level of orbit accuracy can be maintained using any combination of the above tracking systems. Orbit determination at the lower altitude, however, is more difficult. As previously discussed, the most recent experience with SLR at the 800 km altitude is that of ERS-1. Undoubtedly the ERS-1 orbit uncertainty would be decreased significantly if more SLR tracking were available, but it is the near continuous coverage provided by radiometric data of the DORIS or GPS systems that is needed to fully cope with the atmospheric drag perturbations. Experience with DORIS at the 800 km altitude comes from tracking of the SPOT-2 satellite, where it is estimated that a radial orbit accuracy of approximately 10 cm rms is attainable (Nouel et al., 1993). Since DORIS provides only range-rate information, it is difficult to calibrate this accuracy without the benefit of an absolute measure of range such as SLR. If DORIS were used to support a follow-on mission in either the T/P or the GEOSAT orbit, the addition of corner cube reflectors is necessary so that SLR data may be used for strengthened orbit and altimeter calibration purposes. While there is little experience with GPS tracking at GEOSAT altitude, the success of its use on T/P is undeniable (Yunck et al., 1993, Bertiger et al., 1994), and improvements in the flight receiver hardware and software in the near term will make it an even more attractive system for the support of future altimeter missions. Projecting the DORIS and the GPS orbit accuracy capability downwards to the GEOSAT altitude is thus an area of interest.

In summary, the achievable radial orbit accuracy for a follow-on mission in the T/P orbit has been established at the 3 cm rms level. Clearly, such unprecedented accuracy should serve as the standard for future altimeter missions. The expected radial orbit accuracy for a follow-on mission in an 800 km altitude orbit, however, has not been established, and achieving an accuracy commensurate with T/P will pose a great challenge. As a result, this investigation focuses on the radial orbit accuracy that can be achieved at this altitude, with the GEOSAT 17-day repeat orbit used as an example. Given the tracking systems available to support such a mission, the orbit accuracy attainable will tend to be dominated by force model errors rather than measurement model errors. Emphasis is thus given to characterizing the effects of force model errors on the estimated radial orbit accuracy, particularly those due to gravity and drag. The importance of global, continuous tracking of the satellite for reduction in these sources of orbit error is demonstrated with simulated GPS tracking data. Effective orbit determination strategies are presented for mitigating the effects of drag errors, and a gravity tuning experiment is carried out to show how the effects of gravity error may be reduced.

Precise Orbit Determination Considerations

Historically, uncertainty in the geopotential has been the largest source of orbit error for oceanographic satellite missions. However, tremendous improvements made specifically for the T/P mission in modeling the static and time-varying components of the gravity field have substantially reduced these errors. As a result, orbit errors due to gravity are roughly equivalent to those due to surface forces at T/P altitude. Such improvement is best illustrated through the rms radial orbit error predicted by the gravity field covariance (Rosborough, 1986). Results for the T/P pre-launch gravity models, TEG-2B (Tapley et al., 1991) and JGM-1 (Nerem et al., 1994), and for the post-launch tuned models, JGM-2 (Nerem et al., 1994) and JGM-3 (Tapley et al., 1994) are provided in Table 2. It is observed that the radial orbit error due to the JGM-2 gravity model, which is the reference model for the T/P precise orbits produced by NASA, is about 2 cm. The JGM-3 model, which is a refinement of the JGM-1 model with additional information from tracking of T/P (SLR, DORIS, and GPS), Stella, Lageos-2, and SPOT-2, yields about 1 cm rms of radial orbit error. The JGM-3 gravity model also yields improvement for the ERS-1 and GEOSAT orbits, with predicted rms radial orbit errors of about 4-5 cm. Such will be the level of pre-launch radial orbit error due solely to the geopotential for a follow-on mission that occupies either of these orbits. Previous gravity model solutions have demonstrated that post-launch tuning of the gravity field can reduce this error, but the level of success depends on the data quality and the ability to separate gravity effects from surface force effects. It should also be noted that additional radial orbit error can be expected from the time-varying component of the gravity field. Bettadpur and Eanes (1994) have shown that at the 1300 km T/P altitude, the rms radial orbit error due to ocean tides is about 1 cm, and increases to about 3 cm at 800 km altitude. These errors may be reduced through improvements of the ocean tide model with altimeter data being obtained from T/P.

Surface forces have also been large sources of orbit error for oceanographic satellite missions, especially atmospheric drag. A major contributor to the T/P orbit precision is the low atmospheric density associated with the 1330 km altitude, as well as the relatively low solar and geomagnetic activity occurring throughout the mission. These elements have combined to provide T/P with a low drag environment favorable for computing very accurate orbits. For example, at the T/P altitude, the atmosphere is very tenuous, and the accelerations due to solar, terrestrial and thermal radiation pressure are one to two orders of magnitude greater (Ries et al., 1992). At the 800 km altitude of GEOSAT and ERS-1, where the atmosphere is much more dense, drag accelerations may exceed those due to radiation pressure. To illustrate these concepts, typical accelerations due to surface forces at both altitudes are provided in Table 3. These accelerations were computed from daily averages for the first day of each month in 1992 and are based on the precise force models used in the UT/CSR orbit determination software. It is observed that at the 1300 km altitude, the acceleration due to drag is much smaller than that due to solar and terrestrial radiation pressure, and that the variation in the drag acceleration from minimum to maximum is usually no more than an order of magnitude. However, at the 800 km altitude, the acceleration due to drag can exceed that due to solar and terrestrial radiation pressure and exhibits very large fluctuations with the maximum being two orders of magnitude greater than the minimum. Despite the fact that the acceleration due to drag is often smaller than that due to radiation pressure, it is drag that has the most dramatic effect on the orbit. Rapid density fluctuations that can occur several times within a day make modeling the effects of atmospheric drag very difficult at low altitudes.

Simulation Description

The simulation performed in this analysis is intended to provide a preliminary assessment of the radial orbit accuracy that can be achieved for a satellite in GEOSAT orbit, with emphasis on the impact of gravity and drag errors and how the tracking system technology can be used to overcome them. The fidelity of the simulation is dependent upon realistic sources of dynamic and measurement model errors, and effort must be made to ensure that the error models are neither overly optimistic nor pessimistic. Thus, it is necessary that the orbit error models be calibrated against those observed in real data analysis. The dynamic and measurement model errors used in this simulation are generated through differences between the models used in the data generation and the data processing. Random stochastic effects are added in the data generation phase. The residual rms radial orbit difference that remains after the data is processed is the radial orbit error. This simulation makes extensive use of the error models developed for GPS applications by Rim et al. (1993). Improvements to some of these error

models were made with updated information from recent satellite missions. Similarly, error models specific to the GEOSAT orbit were developed for this analysis with knowledge gained from the processing of real satellite data, especially T/P and SPOT-2.

Calibration of the dynamic error model is carried out by integrating the spacecraft equations of motion with the reference force model and then processing the resulting satellite states as observations in a batch filter. This is equivalent to having continuous, perfect observations of the spacecraft position, or "idealized" tracking, and thus considers only force model errors. For example, gravity model error can be simulated by generating a satellite ephemeris using the JGM-1 gravity model, and then processing the resulting satellite positions with the JGM-2 model. Adjusting only the satellite epoch state provides an estimate of the power of a particular source of error, which in this case is the error implied by differences between JGM-1 and JGM-2. Adjusting additional parameters over various arc lengths provides insight into parameterizations that are helpful in absorbing or accommodating such errors. It is this effort to properly calibrate the dynamic model error that receives the most attention in this study, because as previously discussed, measurement errors are not expected to be major contributors to the overall orbit error for the tracking system(s) being considered. Most of the measurement model errors were generated based on uncertainties obtained from the current literature.

The GPS measurement assumed for the simulation was the dual-frequency carrier phase observable in the double-differenced mode. Effects of selective availability, multi-path, phase center migration and ionospheric dispersion on the radial orbit accuracy are neglected. Assumptions for the flight receiver and the ground network are summarized in Table 4. Furthermore, it was assumed that a GPS flight receiver capable of tracking all GPS satellites in view will be available to support the orbit determination.

An assumption on the satellite design is also necessary because knowledge of physical attributes such as the area-to-mass ratio and solar array size are necessary to properly scale the surface forces acting on the satellite. Physical descriptions of some relevant satellites are provided in Table 5. It is observed that the T/P, SPOT-2 and ERS-1 designs are similar in maximum area-to-mass ratio. These satellites are configured in a "box-and-wing" design, where the spacecraft is treated as a combination of flat plates arranged in the shape of a box with an attached solar array. The SPOT-2 model was chosen for the 800 km altitude option because its satellite bus is very similar to the ERS-1 design but does not have the large synthetic aperture radar antenna. The smaller solar panel is also more appropriate because it is unlikely that the follow-on mission satellite will have as large a power requirement as ERS-1.

Error Model Description

The important sources of dynamic model error for any oceanographic satellite are gravitational and surface forces, and at GEOSAT altitude, the atmospheric drag error model is particularly important. Gravitational errors included a bias in the knowledge of the Earth's gravitational coefficient, GM, errors in the geopotential and ocean tide model coefficients, and a bias in the dynamic solid Earth tide parameter. The errors for the geopotential are based on JGM-2 and TEG-2B gravity model differences, and the errors for the ocean tide model are based on differences between selected ocean tide models.

Non-gravitational errors for both the altimeter satellite and the GPS satellites included solar, terrestrial and thermal radiation pressure and atmospheric drag. Such errors are much different for the GPS satellites, compared to a satellite in GEOSAT orbit, because at the 20,000 km altitude of the GPS constellation, the dominant sources of non-gravitational error are direct solar radiation and thermal imbalances, particularly during periods of eclipsing of the Sun by the Earth. The complete dynamic error model employed in this simulation is summarized in Table 6.

The important sources of observational error include instrument noise, clock errors, and media biases due to tropospheric refraction and ionospheric dispersion. Reference frame errors also contribute to the measurement model error, and include errors in the Earth orientation parameters, nutation and precession errors, and station coordinate errors. The basic data type assumed was the GPS dual-frequency carrier phase measurement in the

double-differenced mode. The effects of clock error including selective availability, multi-path, phase center migration and ionospheric dispersion were neglected. Table 7 summarizes the measurement model errors.

Error Model Calibration

As previously discussed, the dynamic error model consists of force model differences between the perturbed orbit and the reference orbit, with random stochastic effects added. The level of orbit error generated in this manner is examined by integrating the spacecraft equations of motion with the reference force model and then processing the resulting satellite states with the perturbed model. Dynamic model parameters are estimated over various arc and sub-arc lengths to absorb the force model errors, and the residual radial orbit differences that remain are compared to the expected level of orbit errors derived from real data experience.

The calibration results for the dynamic error model is given in Table 8, where the dominant error sources are examined individually. For each case considered, a ten day ephemeris was generated with five minute spacing. Two arc epochs were utilized to highlight the effects of low and high atmospheric activity on the drag error model. The ephemeris was processed such that the satellite state was adjusted once over the entire ten day arc, and the empirical 1-cpr transverse (T) and normal (N) parameters were adjusted for each day. In the case of the GEOSAT error model calibration, drag scaling parameters were adjusted every six hours, while for T/P, along-track accelerations (C_T) were adjusted every six hours.

In Case 1, the gravity error due to JGM-2 and TEG-2B differences is examined. The model differences for these two fields are much too large to be realistic at T/P altitude, but appear to generate very realistic radial orbit errors for GEOSAT altitude. As given in Table 2, the rms radial orbit error predicted from the JGM-2 covariance is 7.4 cm, and residual rms orbit error obtained with the model differences yields the same result. In Case 2, the gravity error due to JGM-2 and JGM-1 differences is examined. These model differences result in 2.1 cm rms radial orbit errors for T/P, which is compared to value of 2.2 cm from the JGM-2 covariance. The 3.6 cm rms radial orbit errors generated for GEOSAT with these model differences is about half of that predicted by the JGM-2 covariance, and is more representative of what tuning the gravity model might provide. Accordingly, the errors generated by the aforementioned model differences will be termed the "pre-launch" and "tuned" gravity model errors. In Case 3, the error due to a bias in GM results in about 0.5 cm of radial orbit error regardless of the orbit altitude. In Case 4, ocean and solid Earth tide errors result in about 3 cm of radial orbit error at GEOSAT altitude. In Case 5, the drag error model was examined. It is observed that drag is negligible at T/P altitude, regardless of the epoch. However, at GEOSAT altitude, the rms radial orbit error increased by more than a factor of three for the highly variable atmosphere of the March, 1991 epoch. Moreover, this level of radial orbit error is about twice as large as the gravity error from the "tuned" model and is commensurate with the gravity error from the "pre-launch" model. In Case 6, the solar, terrestrial, and thermal radiation pressure error model is examined. It is observed that level of rms radial orbit error, which was generated from a fairly pessimistic error model, is small in comparison to both the gravity and the drag error. This again demonstrates the ability of the empirical accelerations to absorb mismodeled or unmodeled accelerations, especially those that have distinct 1-cpr signatures such as radiation pressure errors.

The aggregate effect of these individual dynamic error sources on the rms radial orbit accuracy is shown in Table 9. The final dynamic error model for GEOSAT orbit was selected to emulate "pre-launch" dynamic errors, and the final dynamic error model for T/P orbit was selected to emulate the current dynamic errors that have been observed in real data processing. The effect of arc length was investigated to illustrate the impact of dynamic model error build-up on the rms radial orbit accuracy. Long arcs, on the order of a few to several days, provide dynamical constraints through the satellite equations of motion, but suffer from the build-up of non-conservative surface force model errors. Short arcs, on the order of a day or less, tend to attenuate long-period and resonant gravity errors and reduce the build-up of non-conservative surface force model errors. For each arc length used, initial conditions were adjusted at arc epoch and C_D's for GEOSAT and C_T's for T/P were adjusted every six hours. The 1-cpr T and N accelerations were adjusted daily, except in Case 4, where they were adjusted every six hours. From Cases 1 through 3, it is observed that for both T/P and GEOSAT shortening the arc length from one ten-day arc to ten one-day arcs has little effect on the rms radial orbit error, although a slight benefit was gained

for GEOSAT in the March, 1991 time frame where the drag model error was greater. It is thus seen that one day arcs essentially contain all the dynamic orbit error that is present in the longer arcs, mainly because of the power of the 1-cpr T and N accelerations in absorbing slowly changing accelerations. This implies that long arcs, such as the ten-day arc length used to generate the precise T/P orbits, can be parameterized in a manner that does not result in significantly increased orbit error relative to one-day arcs. In Case 4, the sub-arc length of the 1-cpr T and N parameters is reduced to six hours, and such a parameterization begins to approach the "reduced dynamic" filtering technique used successfully with GPS data on T/P (Bertiger et al, 1994). It is observed that the parameterization in Case 3 results in a significant reduction in the rms radial orbit error generated for both GEOSAT and T/P in the February, 1993 time frame, and for T/P in the March, 1991 time frame. However, only a negligible reduction in the March, 1991 time frame was realized for GEOSAT, indicating that additional C_D's are needed to further reduce the drag error. For T/P, it is observed that the time frame of the simulation has little impact on the rms radial orbit error, indicating the drag model error is not a major consideration for this high altitude. Finally, it is observed that the dynamic error model yields rms radial orbit errors for GEOSAT orbit at the 8-9 cm level for a benign atmosphere and at the 9-11 cm level for a volatile atmosphere when arc lengths of one day or longer are used.

GPS Error Model Calibration

Calibration of the GPS error model was carried out by comparing the data fits for the simulated GPS data with those observed in real GPS data processing. This was done using GPS data collected during a twelve-day period beginning February 2, 1993. Orbits were obtained for the GPS satellites using two different parameterizations, one utilizing the classical approach and the other utilizing the empirical acceleration parameters. In both cases, the twelve days of data were processed in four three-days arcs. In the first case, initial conditions, a Y-bias parameter and a scale factor for the box-wing radiation pressure model were adjusted at arc epoch. The real and simulated data fits showed excellent agreement, with residuals on the order of 2.2 to 2.5 cm. The smallest difference in residual rms observed between the real and simulated data fits was 0.01 cm, and the largest was 0.1 cm. In the second case, initial conditions, a C_T and a 1-cpr T and N were adjusted at arc epoch. The real and simulated data fits again showed excellent agreement, with residuals on the order of 1.4 to 1.6 cm. The smallest difference observed was 0.02 cm and the largest difference was 0.12 cm. In either case, the simulated data did not fit consistently below that of the real data, indicating the error models are not too optimistic. In Tables 10 and 11, one-day orbits are compared against the three-day orbits discussed above using the Y-bias and radiation pressure scale factor parameterization. The similarities between the results is striking, especially considering the agreement for GPS satellites 2 and 20 which were being eclipsed by the Earth. Thus the dynamic error model used for the GPS component of this simulation emulates quite well that which is observed in real data processing.

Simulation Results

Eighteen days of GPS double-differenced phase data were simulated for a SPOT-2 type satellite in the GEOSAT orbit beginning February 2, 1993 with the comprehensive dynamic and measurement error models previously described. The epoch was selected to provide atmospheric conditions conducive to the separation of drag effects from gravity effects, so the results will be somewhat optimistic. To test the effectiveness of tuning the gravity field for a satellite in this orbit, information equations from the first twelve days of the data were obtained with four three-day arcs. This provided six days of data withheld from the tuned field for comparison purposes. Orbits for the altimeter satellite and all GPS satellites were adjusted simultaneously along with the positions of twelve of the fifteen GPS ground stations. The three stations with the smallest random position errors were held fixed as fiducial sites. The parameterization used for the altimeter satellite was six-hour C_D's and a daily 1-cpr T and N, while that for the GPS satellites was a daily Y-bias and a three-day C_R. Recall that JGM-2 is the reference gravity field and TEG-2B is the field used to generate gravity errors through the model difference. The recovery of the JGM-2 field in this experiment is shown by plotting the degree difference variance (DDV) in Fig. 1. The heavy line with solid dots represents the DDV of TEG-2B with respect to JGM-2, and the dashed lines with open dots represents the DDV of the tuned field. If the JGM-2 gravity field were perfectly recovered, the DDV would be zero for all degrees. It is observed that TEG-2B and JGM-2 agree well for the dominant zonal terms such as J_2,

J_3, etc., but that the differences become large for degrees above four. Partial recovery of the JGM-2 model is obtained in the tuning process for degrees up to about 24, with much of the improvement attributed to the resonant terms. Above degree 24, the DDV of the tuned field surpasses that of TEG-2B until about order 38, suggesting that some of the surface force errors may have slightly contaminated the gravity model. When all eighteen days of data are included in the gravity model, the results were essentially the same. This demonstrates that tuning the gravity field with the satellite tracking data is effective in reducing the radial orbit error due to the geopotential, particularly that which is attributed to the low degree and order terms. Only twelve days of tracking data were used to tune the gravity field in this experiment, so further improvement could be realized with the additional information provided by a few months of data. This would provide the much needed data redundancy required to average out the random components of the surface force model errors.

The results obtained from processing the simulated GPS double-differenced phase data with the pre-tuned and tuned gravity models are given in Table 12. The eighteen days of data were processed in six three-day arcs using the daily Y-bias and three-day radiation scale factor parameterization for the GPS satellites, and the six-hour C_D and daily 1-cpr T and N parameterization for the altimeter satellite. It is observed that for the pre-tuned field, the rms of the double-differenced phase residuals is on the order of 5-7 cm, and is subsequently reduced to 3-5 cm rms with the post-tuned field. It is interesting to note that although the last two three-days arcs were not used to tune the gravity field, improvement in those residuals was still obtained. Furthermore, comparison of the best fit orbits to the reference orbit shows that radial orbit errors of about 8-11 cm rms are generated with the pre-tuned gravity field and all other dynamic and measurement errors, while about 6-7 cm rms error are generated with the post-tuned field. The reduction in rms radial orbit error due to gravity tuning is thus significant, especially when it is considered that only twelve days of a single 17-day GEOSAT repeat orbit was used for the tuning. Further improvement is obtained when one-day arcs are used to reduce the contribution of drag error, as shown in Table 13. It is observed that for both the pre-tuned and post-tuned cases, the residuals are reduced roughly by half when one-day arcs were used. The reduction in rms radial orbit error is about the same for both cases, indicating that short arcs on the order of one day may be needed to contend with the level of drag error associated with the GEOSAT altitude.

Conclusions

A study was conducted to predict the rms radial orbit error that could be achieved for an altimeter satellite in GEOSAT orbit being tracked by GPS. The numerical simulation technique was used to generate realistic sources of orbit error with dynamic and measurement error models calibrated with knowledge from real data processing. The GPS tracking scenario assumed a constellation of 21 Block II satellites, with flight and ground receivers that can track all GPS satellites in view. A gravity tuning experiment was conducted to demonstrate how the rms radial orbit error due to the geopotential can be reduced, and orbit determination tests were conducted to examine strategies effective in reducing the atmospheric drag error. From this study, it was found that the expected radial orbit error due solely to the geopotential can be reduced with post-launch tuning of the gravity field. Only twelve of the eighteen days of simulated tracking data were used to tune the field, yet a significant reduction in the radial orbit error was obtained. The radial orbit error due to drag, however, will be more difficult to mitigate. The simulation results suggest that, in a low drag environment and with a tuned gravity field, about 5 cm of rms radial orbit error can be expected when one-day arcs are used. This also assumes that robust tracking is provided by a GPS flight receiver capable of tracking all GPS satellites in view. The dynamic error model calibration showed that the drag error can increase substantially when high atmospheric density variations exist. Adjusting the geopotential model in this high-drag environment will be more difficult and is a topic for further study.

Acknowledgments

The research was prepared under NASA contract JPL-959737. Additional computing resources were provided by the University of Texas System Center for High Performance Computing.

References

Bertiger, W. I., Y. E. Bar-Sever, E. J. Christensen, E. S. Davis, J. R. Guinn, B. J. Haines, R. W. Ibanez-Meier, J. R. Jee, S. M. Lichten, W. G. Melbourne, R. J. Muellerschoen, T. N. Munson, Y. Vigue, S. C. Wu, T. P. Yunck, B. E. Schutz, P. A. M. Abusali, H. J. Rim, M. M. Watkins, and P. Willis, GPS precise tracking of TOPEX/POSEIDON: Results and implications, submitted to *J. Geophys. Res.*, 1994.

Bettadpur, S. and R. J. Eanes, A tidally coherent geographically correlated representation of orbit error due to ocean tide model error, submitted to *EOS Trans. AGU*, Spring, 1994.

Chambers, D. P., C. K. Shum, J. C. Ries, and B. D. Tapley, Precise ephemerides for the Geosat exact repeat mission, manuscript in preparation, Center for Space Research, The University of Texas at Austin, 1994.

Fu, L. L., E. J. Christensen, M. Lefebvre, and Y. Menard, TOPEX/POSEIDON mission overview, submitted to *J. Geophys. Res.*, 1994.

Kozel, B. J., C. K. Shum, J. C. Ries, and B. D. Tapley, Precision orbit determination using dual satellite altimeter crossover measurements, *Proc. of AAS/AIAA Spaceflight Mechanics Meeting,*, Cocoa Beach, Florida, February 1994.

Nerem, R. S., F. J. Lerch, J. A. Marshall, E. C. Pavlis and B. H. Putney, J. C. Chan, S. M. Klosko, S. B. Luthcke, G. B. Patel, N. K. Pavlis, R. G. Williamson, B. D. Tapley, R. J. Eanes, J. C. Ries, B. E. Schutz, C. K. Shum, and M. M. Watkins, R. H. Rapp, R. Biancale and F. Nouel, Gravity model development for TOPEX/POSEIDON: Joint Gravity Model-1 and 2, to appear *J. Geophys. Res.*, 1994.

Nouel, F., J. Bardina, C. Jayles, Y. Labrune, and B. Troung, DORIS : A precise satellite positioning doppler system, Astrodynamics 1987, *Adv. Astron. Sci.*, J. K. Solder et al. (Eds.), 65, 311-320, 1988.

Nouel, F., M. Deleuze, C. Valorge, P. Laudet, Improvement of the ERS-1 orbit precision by using the drag effect on SPOT-2, *Proc. of. AAS/AIAA Astrodynamics Specialist Conference*, Victoria, B. C., Canada, August 1993.

Rim, H. J., B. E. Schutz, B. D. Tapley, Error modeling for GPS geodetic applications, *Proc. of AAS/AIAA Spaceflight Mechanics Meeting,*, Pasadena, California, February 1993.

Ries, J. C., C. K. Shum, and B. D. Tapley, Surface force modeling for precision orbit determination, *Environmental Effects on Spacecraft Positioning and Trajectories*, Geophysical Monograph 73, IUGG Vol. 13, 1993.

Rosborough, G. W., Satellite orbit perturbations due to the geopotential, CSR-86-1, Center for Space Research, The University of Texas at Austin, 1986.

Tapley, B. D., C. K. Shum, D. N. Yuan, J. C. Ries, R. J. Eanes, M. M. Watkins, and B. E. Schutz, The University of Texas Earth gravitational model, XX General Assembly of the IUGG, Vienna, Austria, August 1991.

Tapley, B. D., J. C. Ries, G. W. Davis, R. J. Eanes, B. E. Schutz, C. K. Shum, M. M. Watkins, J. A. Marshall, R. S. Nerem, B. H. Putney, S. M. Klosko, S. B. Luthke, D. Pavlis, R. G. Williamson, and N. P. Zelensky, Precision orbit determination for TOPEX/POSEIDON, submitted to *J. Geophys. Res*, 1994.

Tapley, B. D. et al., The JGM-3 gravity model, manuscript in preparation, Center for Space Research, The University of Texas at Austin, 1994.

Yunck, T. P., W. I Bertiger, S. C. Wu, Y. Bar-Sever, E. J. Christensen, B. J. Haines, S. M. Lichten, R. J. Muellerschoen, Y. Vigue, and P. Willis, First assessment of GPS-based reduced dynamic orbit determination on TOPEX/POSEIDON, to appear in *Geophys. Res. Lett.*, 1993.

Table 1. TOPEX/Poseidon Orbit Error Budget

Error Source	Mission Specification (cm)	POE Estimate (cm)
Gravity	10	2
Radiation pressure (solar, terrestrial, thermal)	6	2
Atmospheric drag	3	1
GM (Earth's gravitational constant)	2	1
Earth and ocean tides	3	1-2
Troposphere	1	< 1
Station positions	2	1
RSS absolute error	**12.8**	**3-4**

Table 2. RMS Radial Orbit Error Predicted by Gravity Covariance

	TOPEX (cm)	ERS-1 (cm)	GEOSAT (cm)
TEG2B	10.1	19.2	15.3
JGM1	3.4	8.3	8.2
JGM2	2.2	7.9	7.4
JGM3	1.0	4.0	5.3

Table 3. Typical Accelerations Due to Surface Forces

Satellite	Altitude (km)	Average Solar Radiation (10^{-9} m/sec^2)	Average Earth Radiation (10^{-9} m/sec^2)	Min / Max Atmospheric Drag (10^{-9} m/sec^2)
T/P	1300	60	3	0.2 / 1.7
GEOSAT/ERS-1	780	70	9	3 / 136

Table 4. GPS Tracking Assumptions

- GPS constellation consists of 21 Block II satellites
- Flight and ground receivers track all GPS satellites in view
- 15^{o} elevation cut-off for ground stations; 5^{o} elevation cut-off for altimeter
- 15 GPS ground stations
- 2 minute observation sampling time

Table 5. Altimeter Satellite Orbit and Spacecraft Geometry

Satellite	Alt. (km)	Inc (deg)	Mass (kg)	Max Area/mass (m^2/kg)	Projected Areas			
					Roll (m^2)	Pitch (m^2)	Yaw (m^2)	Solar Panel (m^2)
T/P	1330	66	2417	0.012	4.7	8.2	8.3	25.5
SPOT-2	820	98.7	1875	0.013	6.5	3.5	9.0	18.5
ERS-1	770	98.5	2400	0.014	5.0	5.0	15.0	28.0
GEOSAT	780	108	662	0.008	5.0			

Table 6. Dynamic Error Models used in Simulation

- Altimeter satellite and GPS gravitational errors :
  - GM error of 0.0008 km^3/sec^2
  - Geopotential errors from JGM-2 vs. TEG-2B
  - Ocean tide errors from CSR tide model differences
  - Solid earth tide errors from 3% error in k_2
- GPS non-gravitational errors :
  - Radiation pressure
    - > box-wing reflectivity randomly perturbed by 5%
    - > thermal acceleration with amplitude of 1 nm/sec^2, on vs. off
    - > 5 km random error in Earth shadow radius
    - > integration step size, 500 sec vs. 600 sec
  - Y-bias acceleration stochastically perturbed by 5%, 6-hour correlation time
  - Constant 1^o solar panel misalignment, constant 1^o solar panel pitch angle error
- Altimeter satellite non-gravitational errors :
  - Radiation pressure
    - > 50% error in solar reflectivity, Earth albedo and emissivity
    - > Earth albedo and emissivity also randomly perturbed by 3%
    - > 50% error in thermal model acceleration and time decay
    - > 5 km random error in Earth shadow radius
    - > integration step size, 50 sec vs. 60 sec
  - Drag error from constant flux, random 3-hour K_p vs. standard flux and K_p
  - Constant 1^o solar panel misalignment, constant 1^o solar panel pitch angle error

Table 7. GPS Measurement Error Model used in Simulation

- Observational Errors :
  - 5 mm random error for each phase range
  - time tag errors from two-point Allan variance model with
    $\sigma_f = 5x10^{-13}$, $\tau_1 = 1x10^3$, $\tau_2 = 1x10^5$ for TPFO receiver
    $\sigma_f = 1x10^{-13}$, $\tau_1 = 1x10^5$, $\tau_2 = 1x10^7$ for GPS ground receivers
  - troposphere error from modified Hopfield model vs. Chao's model, with 0.8% stochastic tropospheric biases added
  - Phase center errors via satellite attitude errors of 1^o in roll, pitch, yaw
- Random precession and nutation errors
  - 0.1 mas/yr random error in precession
  - 1.0 mas noise in 1-day values of nutation
  - 0.1 mas random errors in long period of nutation
  - 0.05 mas random errors in short period components of nutation
- 1 mas random noise in 5-day values of Earth orientation (x_p, y_p, UT1)
- 3 cm random errors in station coordinates
- 3% random errors in individual station tide corrections
- 8 mm/yr random error in all tectonic plate velocities

Table 8. Altimeter Satellite Dynamic Error Model Calibration Using 10-Day Arcs

		RMS Radial Orbit Differences (cm)			
		Epoch 2/1/93		Epoch 3/12/91	
Case	Error Source	T/P	Geo	T/P	Geo
1	"pre-launch" gravity model error	n/a	7.4	n/a	7.4
2	"tuned" gravity model error	2.1	3.6	2.1	3.7
3	GM error	0.5	0.5	0.5	0.5
4	ocean and solid Earth tide error	1.0	3.4	1.2	3.3
5	atmospheric drag error	0.0	1.8	0.1	7.1
6	radiation pressure error	0.2	0.7	0.1	0.5

Table 9. Final Altimeter Satellite Dynamic Error Model Calibration

	RMS Radial Orbit Differences (cm)			
	Epoch 2/1/93		Epoch 3/12/91	
Case	T/P	Geo	T/P	Geo
1	2.4	8.9	2.4	10.6
2	2.4	8.6	2.4	10.1
3	2.3	8.1	2.3	9.5
4	1.6	6.7	1.5	9.4

Table 10. Error Model Calibration for GPS Satellites
3-day vs. 1-day Orbit Solution Differences using Real Data

GPS Satellite	Radial RMS (m)	Transverse RMS (m)	Normal RMS (m)	RSS (m)
1	0.2634	0.7123	0.3910	0.8541
2	0.4284	1.1245	0.5433	1.3203
3	0.2510	0.5016	0.3004	0.6363
11	0.1980	0.6501	0.3796	0.7784
12	0.2324	0.6680	0.3091	0.7719
13	0.2008	0.5326	0.2975	0.6422
14	0.2656	0.5521	0.2726	0.6705
15	0.2764	0.8046	0.4113	0.9450
16	0.2787	0.8108	0.3393	0.9220
17	0.3383	0.8126	0.3526	0.9482
18	0.1738	0.4004	0.2630	0.5096
19	0.1763	0.4771	0.2488	0.5663
20	0.4459	1.2239	0.4165	1.3676
21	0.2743	0.7410	0.2823	0.8390
23	0.1971	0.5730	0.2962	0.6745
24	0.2967	0.7115	0.3656	0.8532
25	0.2668	0.8509	0.3786	0.9688
26	0.2118	0.6973	0.3655	0.8153
27	0.2113	0.6229	0.3151	0.7293
28	0.2606	0.7045	0.3521	0.8296
29	0.2735	0.5825	0.3535	0.7342

Table 11. Error Model Calibration for GPS Satellites
3-day vs. 1-day Orbit Solution Differences using Simulated Data

GPS Satellite	Radial RMS (m)	Transverse RMS (m)	Normal RMS (m)	RSS (m)
1	0.2021	0.6088	0.3536	0.7325
2	0.4454	1.2733	0.5832	1.4696
3	0.2526	0.5433	0.3302	0.6841
11	0.1878	0.6441	0.3184	0.7427
12	0.1812	0.5483	0.2990	0.6503
13	0.1578	0.4224	0.2212	0.5022
14	0.2369	0.4815	0.2404	0.5880
15	0.2699	0.7739	0.3912	0.9082
16	0.2676	0.7449	0.2984	0.8459
17	0.3427	0.8260	0.3077	0.9457
18	0.1478	0.3470	0.2635	0.4601
19	0.1744	0.5760	0.2775	0.6627
20	0.4916	1.3548	0.4643	1.5142
21	0.2638	0.6340	0.3163	0.7561
23	0.1737	0.5282	0.2835	0.6241
24	0.2604	0.6162	0.3105	0.7375
25	0.2409	0.8529	0.4322	0.9860
26	0.1459	0.6022	0.3692	0.7213
27	0.2017	0.6303	0.3061	0.7291
28	0.2911	0.8480	0.3687	0.9695
29	0.2651	0.5459	0.3443	0.6978

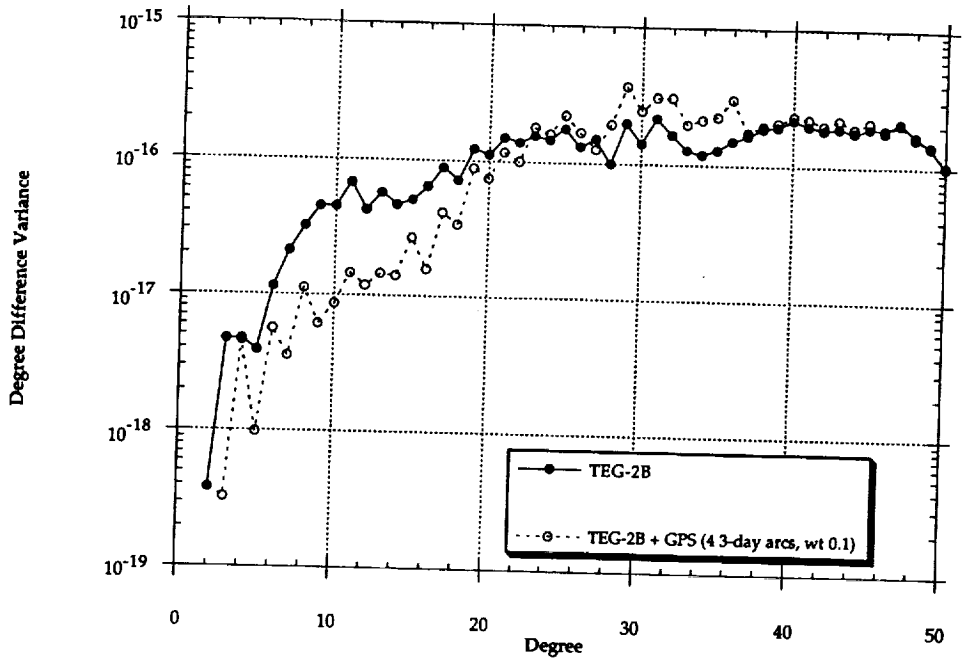

Fig. 1 GPS-Tuned Geopotential Model Evaluation

Table 12. Results of GPS Tuning Experiment using 3-day Arcs (solar activity of 2/1/93)

	Pre-Tune				Post-Tune			
	Residual RMS (cm)	RMS Orbit Differences (cm)			Residual RMS (cm)	RMS Orbit Differences (cm)		
Arc		R	T	N		R	T	N
1	5.7	8.7	34.1	17.4	3.6	5.9	17.3	7.9
2	5.5	9.8	29.6	22.9	4.0	6.2	18.4	10.8
3	6.2	10.8	37.8	20.6	4.0	6.7	17.1	7.2
4	7.0	10.0	42.8	21.4	4.6	6.5	19.8	13.2
5	6.2	7.5	40.0	17.6	4.5	5.9	22.3	8.0
6	5.5	7.9	27.5	15.5	4.8	6.8	27.4	8.6

Table 13. Results of GPS Tuning Experiment using 1-day Arcs (solar activity of 2/1/93)

Pre-Tune				Post-Tune			
Residual RMS (cm)	RMS Orbit Differences (cm)			Residual RMS (cm)	RMS Orbit Differences (cm)		
	R	T	N		R	T	N
3.3	8.2	25.5	18.5	1.8	4.5	12.6	8.6